Efficient Numerical Simulation of a One-Dimensional Electrothermal Deicer Pad

R. J. Roelke,*
NASA Lewis Research Center, Cleveland, Ohio
and
T. G. Keith Jr.,† K. J. DeWitt,‡ and W. B. Wright§
University of Toledo, Toledo, Ohio

In this paper, a new approach to calculate the transient thermal behavior of an iced electrothermal deicer pad is developed. The method of splines is used to obtain the temperature distribution within the layered pad. Splines are used in order to create a tridiagonal system of equations that can be directly solved by Gauss elimination. The Stefan problem is solved using the enthalpy method along with a recent implicit technique. Only one to three iterations were needed to locate the melt front during any time step. Computational times were shown to be greatly reduced over those of an existing one-dimensional procedure without any reduction in accuracy; the current technique was more than 10 times faster.

Nomenclature

A = coefficient of the X_{j-1} term in Eq. (23)
B = coefficient of the X_j term in Eq. (23)
c_p = specific heat
C = coefficient of the X_{j+1} term in Eq. (23)
C_H = coefficient in enthalpy function
C_θ = coefficient in the Kirchhoff temperature function
D = right hand side of Eq. (23)
h = grid spacing and convective coefficient
H = enthalpy per unit volume
J = last grid point in layer
k = thermal conductivity
L = latent heat of fusion
m = first derivative of the spline function
M = second derivative of the spline function
q'' = heat flux
r = Fourier number
$S(x)$ = spline function
t = time
T = temperature
$u(x)$ = arbitrary function
x = coordinate dimension
X = arbitrary scalar or vector variable in Eq. (23)
α = thermal diffusivity
ϵ = slope constant in phase property relations
ρ = density
θ = Kirchhoff variable

Superscripts

n = time level
T = transpose

Subscripts

i = layer index
I = interface
j = spatial node index
l = liquid phase
m = melting point
R = reference value
s = solid phase
w = two-phase substance

Presented as Paper 87-0024 at the AIAA 25th Aerospace Sciences Meeting, Reno, NV, Jan. 12-15, 1987; received April 5, 1987; revision received May 31, 1988.

*Aerospace Engineer.
†Professor. Associate Fellow AIAA.
‡Professor.
§Graduate Assistant.

Introduction

OVER the past few years, finite-difference methods have been used in numerical investigations of the flow of heat in multilayered bodies. The top of the body is covered with a layer of ice and one of the internal layers contains discrete heat sources (heaters) distributed along the layer. Interest in this problem stems from the fact that such a composite structure is found in an electrothermal deicer pad that is used for removing ice from exposed surfaces of aircraft components. A comprehensive description of the deicer pad and how it compares to other deicing and anti-icing methods may be found in Ref. 1.

Deicer Pad Models

Predicted transient behavior of an electrothermal deicer pad has been obtained using one- and two-dimensional heat transfer analyses. In the one-dimensional studies[1-5] there are no gaps between the heat sources and all layers, including the ice, have uniform properties and thickness. Thus, only a linear slice of the composite needs to be considered. In a recent paper, Leffel et al.[6] compared one-dimensional predictions, using the computer code developed by Marano,[5] to experimental data obtained from a series of tests performed in the NASA Lewis Icing Research Wind Tunnel. In general, the one-dimensional predictions compared favorably with the experimental data. However, in regions of high blade curvature or at locations affected by changes in layer structure (e.g., in gaps between heaters, at extremities of the ice layer, at changes in layer materials, etc.), replacement of the one-dimensional models with two-dimensional versions should be considered.

Several two-dimensional numerical investigations of an electrothermal deicer pad have appeared.[2,7-11] The two-dimensional models have taken two forms: a segmented heater form, written in a Cartesian coordinate system, and a full-blade

form, written in a nonorthogonal coordinate system. In the first type,[2,7,8] the heaters are assumed to be evenly spaced and transient behavior is determined for only a section of the pad. In the full two-dimensional model,[9-11] effects of geometry, including blade curvature and ice shape, are taken into account by a coordinate mapping procedure.

As may be expected, as the modeling becomes geometrically more involved, the required computational times increase substantially. It has been found that the computational times of the full two-dimensional simulation are roughly an order of magnitude larger than those of the section two-dimensional simulation and two orders of magnitude beyond those of the one-dimensional simulation. Clearly, for these methods to have practical design utility, the computational times must be restricted to values that permit a number of cases to be considered in a realistic time frame. Unless this condition is satisfied, these methods would hardly ever be used as design tools.

To avoid this possibility, it was decided to investigate methods for reducing the computational times of the various deicer pad models. Because the one-dimensional version model is easiest to work with, and was thought to be the most difficult to speed up, it was used in this paper to demonstrate the potential for improving computational efficiency. It should be noted that this improvement was sought without requiring fewer grid points and/or using larger time steps, or resorting to the use of more powerful computers.

In considering how to enhance the computational efficiency of the numerical treatment of a deicer pad, attention may be directed toward two principal aspects of the solution procedure: 1) the method used to model the heat transfer within the various layers of the composite, and 2) the method used to model the change of phase of the ice.

Cubic Splines

Many approaches are available to handle the internal heat transfer computation. For this study, the method of cubic splines was selected. There are several advantages that may be realized by applying cubic splines to the numerical solution of the internal deicer pad heat-transfer problem. These include:

1) The computational grid need not be uniform and there is no loss of accuracy associated with the use of a variable mesh.

2) The boundary conditions may be readily incorporated into the solution procedure and there is no need to first represent these conditions in finite-difference form.

3) The governing equations and boundary conditions may be turned into a tridiagonal system of algebraic equations and efficiently solved using Gauss elimination.

4) The interpolating properties of splines may be exploited to obtain values at locations that lie between node points.

The method of splines has been used in the numerical solution of a variety of engineering problems. The theory and use of splines was developed by Ahlberg et al.[12] Examples using this technique were given by Davis and Rabinovitz.[13] Paramichael and Whiteman[14] applied the spline technique to the solution of a one-dimensional heat conduction problem that did not include phase change. Rubin and Graves[15] used splines to solve a number of fluid flow problems. Recently, Lin et al.[16] utilized the spline method in an abalation problem, but did not track the transient behavior of the melt front.

Applying the method of splines to the situation where phase change can occur required additional considerations. The spline method is relatively easy to apply if the material properties do not depend upon the temperature. However, for a substance undergoing a phase change this is not the case. To overcome this difficulty, a Kirchhoff temperature transformation, as described in Arpaci,[17] was used.

Phase Change Modeling

To avoid the difficult task of determining the spatial location of the phase change front, the so-called enthalpy method[18] can be applied to the melting region. Enthalpy methods have been frequently used to obtain numerical solutions of moving phase front problems. Such problems are called Stefan problems.

Enthalpy methods present at least two major difficulties.[19] The first deals with accuracy of the method, for it is well known that solution accuracy depends on the position of the phase front. However, these inaccuracies have been resolved by Voller and Cross.[20] The second difficulty arises because the descretized equations for any implicit scheme applied to the method produce a set of nonlinear algebraic equations that generally require a time-consuming iteration procedure to solve. This negates one of the major advantages of the spline method. However, Schneider and Raw[21,22] recently proposed a method that can overcome this obstacle. By their method, the state of each node in the phase change region is assumed at each time step. This reduces the number of unknowns and permits the resulting system of algebraic equations to be tridiagonal in form. The equations can then be efficiently solved, after which the starting assumption regarding the state of all the nodes is updated. Thus, the method acts more as a predictor-corrector scheme than an iterative procedure. In this paper, this implicit procedure will hereafter be referred to as the method of assumed states.

Neither cubic splines nor the method of assumed states have been used in any of the previous deicer models. Applying these numerical techniques to reduce the computational times of the electrothermal deicer pad heat-transfer analysis is the subject of this paper.

Analysis

Physical Considerations

A section of the composite structure used for the analysis is shown in Fig. 1. It consists of four layers plus the accreted ice. The bottom layer is the load-carrying substrate. The external surface of the substrate is subjected to a convective heat exchange. The internal surface of the substrate is covered with a layer of insulation. The heater is sandwiched between two layers of insulation. The bottom insulating layer is much thicker than that of the top so that most of the generated heat is directed toward the ice. A metal shield covers the top layer of insulation for protection. The insulating layers electrically isolate the heater from the metal substrate and the abrasion shield. The layers of the composite are joined to each other

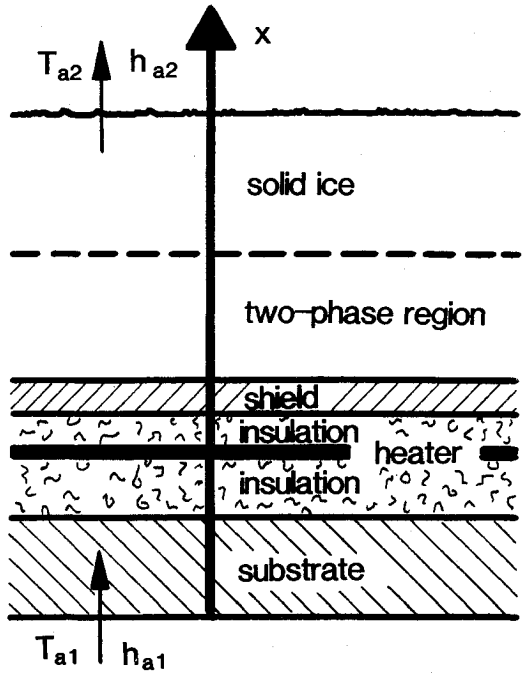

Fig. 1 One-dimensional model of an iced electrothermal deicer pad.

with adhesive. The adhesive was not modeled in the analysis, but could be easily included as additional layers with their own thermal properties. The heater is usually very thin (approximately 1-5/1000-in. thick), and therefore was treated as having zero thickness (a point heater). The ice surface exposed to the ambient is subjected to convective heat transfer different from that of the substrate.

Analytical Considerations

The following assumptions were used to develop an analytical model of the physical problem previously described:

1) The heat flow direction is exclusively from the heater to the ice layer and/or the substrate so that the problem can be considered in terms of a single spatial dimension.
2) There is perfect contact between each of the pad layers.
3) The physical properties of the materials of the composite structure are independent of temperature.
4) The heating element has zero thickness.
5) The convective heat transfer coefficients are constant.
6) The ice has a uniform thickness and is free of impurities.

Internal Layers

The governing energy equation for the ith layer of the composite is

$$(\rho c_p)_i \frac{\partial T_i}{\partial t} = k_i \frac{\partial^2 T_i}{\partial x^2} \qquad i = 1,\ldots,N \tag{1}$$

where $i = N$ corresponds to the abrasion shield and $i = 1$ to the substrate. At the bottom surface of the substrate, for the coordinate system shown in Fig. 1, the convective heat transfer boundary condition is

$$k_1 \frac{\partial T_1}{\partial x}(0,t) = h_{a1}\,[T_1(0,t) - T_{a1}] \tag{2}$$

At the interface between adjacent layers, which are designated by I in the following, temperatures and heat fluxes are continuous, thus,

$$T_i(x_{iI},t) = T_{i+1}(x_{iI},t)$$

$$k_i \frac{\partial T_i}{\partial x}(x_{iI},t) = k_{i+1} \frac{\partial T_{i+1}}{\partial x}(x_{iI},t) \tag{3}$$

At the heater interface, Eq. (3) is modified to account for the flux of heat from the heat source

$$k_2 \frac{\partial T_2}{\partial x}(x_{2I},t) = k_3 \frac{\partial T_3}{\partial x}(x_{2I},t) + q'' \tag{4}$$

Various types of heater outputs can be specified.

Ice Layer

The governing equation and boundary conditions for the ice layer are treated differently from those of the internal pad layers. In particular, Eq. (1) is rewritten in terms of the enthalpy per unit volume, $H = \rho c_p\, T$.

$$\frac{\partial H_w}{\partial t} = \frac{\partial}{\partial x}\left[k_w(T_w)\frac{\partial T_w}{\partial x}\right] \tag{5}$$

This equation is nonlinear and not in the proper form for subsequent application of the spline method. However, it can be made linear by applying the Kirchhoff transformation in which the temperature is replaced by the so-called Kirchhoff variable defined by

$$\theta \equiv \frac{l}{k_R}\int_{T_R}^{T_w} k_w(T)dT \tag{6}$$

In this expression, k_R and T_R are the reference thermal conductivity and temperature, respectively. Direct application of the transformation yields

$$\frac{\partial H_w}{\partial t} = k_R \frac{\partial^2 \theta}{\partial x^2} \tag{7}$$

The enthalpy of a two-phase region is related to the temperature in the following manner and diagrammed in Fig. 2:

$$H = \begin{cases} (\rho c_p)_s T_w, & T_w < T_m \\ (\rho c_p)_s T_m, & T_w = T_m \\ \rho_l[(c_p)_s T_m + L], & T_w = T_m \\ \rho_l[(c_p)_s T_m + L] + (\rho c_p)_l (T_w - T_m), & T_w > T_m \end{cases} \tag{8}$$

Thermal conductivity of water is piecewise continuous about its melt temperature. For a sufficiently small temperature range of about 492°R, the following values may be used:

$$k_w = \begin{cases} 1.416 & T_w \le T_m \\ \text{Btu/h-ft-°F} & \\ 0.320 & T_w > T_m \end{cases}$$

Substituting the above values into Eq. (6), choosing reference values of $T_R = 450$°R and $k_R = 1.416$ Btu/h-ft-°F, and performing the integration, provides the relationships between the temperatures and the Kirchhoff variable in the two-phase region:

$$\theta(T_w) = \begin{cases} T_w - T_R, & T_w < T_m \\ T_m - T_R, & T_w = T_m \\ T_m - T_R + 0.226(T_w - T_m), & T_w > T_m \end{cases} \tag{9}$$

The inverse of this is:

$$T_w(\theta) = \begin{cases} \theta + 450, & T_w < T_m \\ 492, & T_w = T_m \\ 4.425\theta + 306.16, & T_w > T_m \end{cases} \tag{10}$$

As an aid to implementing the method of assumed states, Eqs. (8) and (9) were rewritten in single equation form. For the enthalpy

$$H_w = H_R + C_H T_w \tag{11}$$

where H_R is the reference enthalpy value and C_H is the temperature coefficient. For the Kirchhoff variable

$$\theta_w = \theta_R + C_\theta T_w \tag{12}$$

The coefficients H_R, C_H, θ_R, and C_θ depend on the particular phase:

For a subcooled solid: $T_w < T_m$

$$H_R = 0, \qquad C_H = (\rho c_p)_s \tag{13a}$$

$$\theta_R = -T_R, \qquad C_\theta = 1 \tag{13b}$$

For the transition phase: $T_w = T_m$

$$H_R = (\rho c_p)_s(1 - 1/\epsilon)T_m, \qquad C_H = (\rho c_p)_s/\epsilon \tag{14a}$$

$$\theta_R = T_m - T_R, \qquad C_\theta = 0 \tag{14b}$$

In Eq. (14), ϵ is a small value whose effect is equivalent to having the phase transition occur over a negligibly small temperature range and characterized by a very large specific heat. The value of ϵ used in this study was 10^{-4}.

For a heated liquid: $T_w > T_m$

$$H_w = \rho_l[(c_p)_s T_m + L] - (\rho c_p)_l T_m, \qquad C_H = (\rho c_p)_l \quad (15a)$$

$$\theta_R = T_m - T_R - k_l T_m/k_R, \qquad C = k_l/k_R \quad (15b)$$

Before the transformed boundary conditions for the ice layer can be described, one other consideration will be advanced. The use of the Kirchhoff transformation precludes mixed boundary conditions. Only boundary conditions that prescribe the temperature or the heat flux on the boundaries are permitted. Since there is a convective boundary condition at the exposed ice surface, the ice layer was divided into two parts, as illustrated in Fig. 1. The portion of the ice layer adjacent to the abrasion shield has the proper boundary conditions for direct application of the Kirchhoff transformation technique and thus requires no further consideration. The outer portion of the ice layer is treated as a solid with constant thermal properties, i.e., it is assumed that the melt front never enters this portion of the ice layer. Thus, no Kirchhoff transformation is required there. This does not restrict the proposed methods for a deicer application, since any accreted ice is generally shed shortly after melting occurs.

At the ice-shield interface, the boundary conditions require that

$$T_4(x_{4I},t) = T_w(x_{4I},t)$$

$$k_4 \frac{\partial T_4}{\partial x}(x_{4I},t) = k_R \frac{\partial \theta}{\partial x}(x_{4I},t) \quad (16)$$

Similarly, the boundary conditions for the interface between the two ice layers are

$$T_w(x_{wI},t) = T_5(x_{wI},t)$$

$$k_R \frac{\partial \theta}{\partial x}(x_{wI},t) = k_5 \frac{\partial T_5}{\partial x}(x_{wI},t) \quad (17)$$

The convective boundary condition for the ice layer-ambient interface is

$$k_5 \frac{\partial T_5}{\partial x}(x_{sI},t) = h_{a2}[T_5(x_{sI},t) - T_{a2}] \quad (18)$$

Numerical Considerations

For a given layer in the composite, let the subscript j indicate a spatial node and n a time level. Further, let T_j^n denote a discrete approximation of $T(x,t)$ at (x_j, t_n). Now, a cubic spline function $S(x_j)$ is said to interpolate to the values T_j^n at the nth time level if $S(x_j)$ equals T_j^n for $j = 1,2,\ldots J$. Then an approximate solution to Eq. (1) can be obtained by replacing the equation with

$$\frac{T_{ij}^{n+1} - T_{ij}^n}{\Delta t} = \alpha_i M_{ij}^{n+1} \quad (19)$$

where $M_j = S''(x_j)$. Note that the derivatives are evaluated at the advanced time level, i.e., a fully implicit scheme is used. Also, the first subscript on each of the variables in Eq. (19), i, indicates the layer, and the second subscript, j, the grid point within the layer. Equation (19) can be reduced to an algebraic equation by using the relationships between $S(x_j)$ and its derivatives. The basic cubic spline relationships needed to accomplish this have been developed in the Appendix and are repeated here for convenience.

$$m_1 = -\frac{h}{3}M_1 - \frac{h}{6}M_2 + \frac{U_2 - U_1}{h} \quad (20)$$

$$\frac{h}{6}M_{j-1} + \frac{2h}{3}M_j + \frac{h}{6}M_{j+1} = \frac{U_{j-1} - 2U_j + U_{j+1}}{h} \qquad j = 2,\ldots J-1 \quad (21)$$

$$m_J = \frac{h}{6}M_{J-1} + \frac{h}{3}M_J + \frac{U_J - U_{J-1}}{h} \quad (22)$$

In these equations, $U_j = S(x_j)$, $m_j = S'(x_j)$, $M_j = S''(x_j)$, and h is the incremental distance Δx between two adjacent grid points. The second derivative in Eq. (19) can now be removed with the use of Eqs. (20-22). The resulting equations will contain only the temperatures and first derivatives at the layer boundaries which are, of course, defined by the boundary conditions.

Using the previous spline functions, three general equations are developed to replace Eq. (19) for a given layer: one for the first node in the layer, one for all the interior nodes, and one for the last node in the layer. The equations are developed first for a solid layer and then for a layer undergoing a change of phase. Moreover, the equations can be written in the following tridiagonal form

$$A_{ij}X_{ij-1} + B_{ij}X_{ij} + C_{ij}X_{ij+1} = D_{ij} \quad (23)$$

Note, for the internal layers, the arbitrary variable $X = T$; for the phase change layer, $X = [H\theta]^T$; for the phase change/solid ice interface, $X = [T\,H\,\theta]^T$. In the analysis which follows, only values of the coefficients A, B, C, and D will be given. In the phase change layer, these coefficients will have the number of components that corresponds to the X variable for that region.

Internal Layers

To develop the equation for the first node, Eq. (20) is solved for M_j and, with $U(x_j)$ replaced by T_j^{n+1}, is substituted into Eq. (19) to obtain

$$\frac{T_{ij}^{n+1} - T_{ij}^n}{\Delta t} = \frac{3\alpha_i}{h_i}\left(-m_{ij}^{n+1} - \frac{h_i}{6}M_{ij+1}^{n+1} + \frac{T_{ij+1}^{n+1} - T_{ij}^{n+1}}{h_i}\right) \quad (24)$$

Next Eq. (19) is rewritten for the $(j+1)$ rst layer, inserted into Eq. (24), the result multiplied by Δt, and rearranged so that all unknown temperatures appear on one side of the equation. This produces the following coefficients for Eq. (23):

$$A_{i1} = 0 \quad (25a)$$

$$B_{i1} = 1 + 3r_i \quad (25b)$$

$$C_{i1} = \tfrac{1}{2} - 3r_i \quad (25c)$$

$$D_{i1} = T_{i1}^n + \tfrac{1}{2}T_{i2}^n - 3r_i h_i m_{i1}^{n+1} \quad (25d)$$

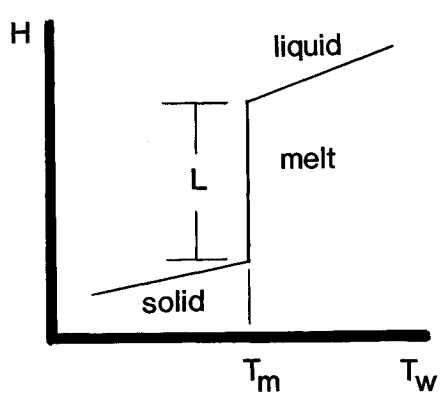

Fig. 2 Temperature enthalpy diagram for water.

where $r_i = \alpha_i \Delta t / h_i^2$ is the dimensionless grid Fourier number. The coefficients in Eqs. (25) inserted into Eq. (23) give the general equation for the initial node of any internal layer. Equation (20) was used for the first node to avoid the introduction of a fictitious node that would lie outside the layer. Also, this equation includes the first derivative through m_j, thus, the boundary condition at the interface is automatically incorporated.

Similar reasoning leads to the selection of Eq. (21) for the interior grid points and Eq. (22) for the last node in the layer. The procedure to develop these equations parallels that used to generate the coefficients in Eqs. (25) and so that development will not be given here. The coefficients to be used in Eq. (23) for the internal nodes and for the ending node of a layer are, respectively,

$$A_{ij} = 1 - 6r_i \quad (26a)$$

$$B_{ij} = 4(1 + 3r_i) \quad (26b)$$

$$C_{ij} = 1 - 6r_i \quad (26c)$$

$$D_{ij} = T^n_{ij-1} + 4T^n_{ij} + T^n_{ij+1} \quad (26d)$$

for $j = 2\ldots,J-1$

$$A_{iJ} = \tfrac{1}{2} - 3r_i \quad (27a)$$

$$B_{iJ} = 1 + 3r_i \quad (27b)$$

$$C_{iJ} = 0 \quad (27c)$$

$$D_{iJ} = \tfrac{1}{2}T^n_{iJ-1} + T^n_{iJ} + 3r_i h_i m^{n+1}_{iJ} \quad (27d)$$

The boundary conditions at the edges of the layers may next be incorporated into the coefficients of Eqs. (25) and (27). Once this is accomplished, these equations together with the interior Eqs. (25) can be used to construct a system of linear algebraic equations for each node of the layered body being analyzed.

The boundary condition at the inner surface of the substrate, i.e., layer 1, grid point 1, is given in Eq. (2) and is rewritten in terms of a spline variable as

$$k_1 m_{11} = h_{a1}(T_{11} - T_{a1})$$

Combining this with Eqs. (25) and rearranging yields the substrate/ambient interface coefficients that are used in Eq. (23)

$$A_{11} = 0 \quad (28a)$$

$$B_{11} = 1 + 3r_i + 3r_i h_1 h_{a1}/k_1 \quad (28b)$$

$$C_{11} = \tfrac{1}{2} - 3r_i \quad (28c)$$

$$D_{11} = T^n_{11} + \tfrac{1}{2}T^n_{12} + 3r_i h_1 h_{a1} T_{a1}/k_1 \quad (28d)$$

For the problem at hand, there are two internal layer interfaces that can be treated in the same manner as that just demonstrated: the interface between the substrate and the lower insulation layer, and the interface between the upper insulation layer and the abrasion shield (refer to Fig. 1). In essence, the procedure is to combine the equations for the last node in the lower layer [Eq. (23) with the coefficients in Eqs. (27)] with the equation for the first node in the layer above it [Eq. (23) with the coefficients in Eqs. (25)] and with the boundary conditions for the interface as described in Eq. (3), written in terms of spline first derivatives m_{ij} and m_{i+1j}. This operation produces an equation that thermally joins together the two adjacent layers and contains within it the physical properties of both layers, as well as the temperatures at and near the interface. The coefficients of Eq. (23) for this interface are

$$A_{ij} = (\tfrac{1}{2} - 3r_i) r_{i+1} h_{i+1}/h_i \quad (29a)$$

$$B_{ij} = (1 + 3r_i)(r_{i+1} h_{i+1}/h_i + r_i k_{i+1}/k_i) \quad (29b)$$

$$C_{ij} = (\tfrac{1}{2} - 3r_{i+1}) r_i k_{i+1}/k_i \quad (29c)$$

$$D_{ij} = \tfrac{1}{2} r_{i+1} h_{i+1} T^n_{ij-1}/h_i + (r_i k_{i+1}/k_i + r_{i+1} h_{i+1}/h_i) T^n_{i+1j} + \tfrac{1}{2} r_i k_{i+1} T^n_{i+1j+1}/k_i \quad (29d)$$

The interfacial equation at the heater is arrived at by the same procedure as that used above. The only difference is the inclusion of the heat flux term. Thus, the following term should be added to D_{ij} in Eqs. (29)

$$3 r_i r_{i+1} h_{i+1} q''/k_i$$

Ice Layer

For the ice layer, Eq. (5) should be used. An implicit finite-difference representation of the equation is

$$H^{n+1}_{wj} - H^n_{wj}/\Delta t = k_R M^{n+1}_{wj} \quad (30)$$

Note that the derivative on the right-hand side of the equation is related to the Kirchhoff variable θ, and not to the physical temperature or the enthalpy, i.e., here the cubic spline function $S(x_j)$ interpolates to θ_j at a given time level.

Proceeding as in the case of an internal layer, the following coefficients may be readily developed for the initial node $j = 1$ in the ice layer $i = w$. Note the variable X in this case is $[H\ \theta]^T$; thus, a set of coefficients having two components are given

$$A_{w1} = [0,0] \quad (31a)$$

$$B_{w1} = [1, 3k_R r_w/\alpha_w] \quad (31b)$$

$$C_{w1} = [\tfrac{1}{2}, -3k_R r_w/\alpha_w] \quad (31c)$$

$$D_{w1} = H^n_{w1} + \tfrac{1}{2}H^n_{w2} - 3k_R h_w r_w m^{n+1}_{w1}/\alpha_w \quad (31d)$$

This is the general expression for the first node in the ice layer and is valid regardless of phase. However, the coefficients take on different value as the phase of the ice changes due to the changing relationship between H and θ, as indicated by Eqs. (8) and (9). Equations (31) are more general forms of Eqs. (25). This may be easily shown by replacing H and θ in Eq. (23) with the coefficients in Eqs. (31) by appropriate expressions for a subcooled solid ($T_w < T_m$) from Eqs. (8) and (9).

The coefficients for the interior and the last node of the portion of the ice layer that may undergo a phase change are developed in a similar manner. Further, the interfacial equations can be developed by uniting the edge boundary conditions with the equations for the first and last grid points in the layer, as was done in the internal layer case. The procedure is direct, but the results are too involved to be presented here. Those developments may be found in Ref. 23.

Computer Implementation

The numerical solution of this problem consists of writing an appropriate equation from the list of interior and interface equations developed for each node of the composite body and ice layer and then solving the system at each time step. In the past, iterative procedures, such as the Gauss-Siedel method, have been employed for problems involving phase change because the physical state reached in the time step is not known prior to the calculation of that time step. The solution at the new time may indeed be in disagreement with the

Table 1 Baseline deicer pad materials and property values

Layer Name	i	Material	Thickness, in.	Thermal conductivity, Btu/ft-h-°R	Specific heat, Btu/lbm-°R	Density, lbm/ft^3
Substrate	1	Aluminum alloy T5S-T6	0.087	66.5	0.230	175.
Insulation (below heater)	2	Epoxy-glass	0.052	0.22	0.230	110.
Insulation (above heater)	3	Epoxy-glass	0.012	0.22	0.230	110.
Shield	4	304 stainless steel	0.012	8.7	0.118	495.
Ice	5	Ice	0.250	1.416	0.502	57.4
		water		0.320	1.00	62.4

Table 2 Comparison of results with reference code

Initial temperature, °F	Heater output, W/in.^{2} 15.0		25.0		40.0	
	Marano[5]	MELT	Marano[5]	MELT	Marano[5]	MELT
23	1.70[a]	1.60	1.00	0.99	0.60	0.65
14	3.70	3.70	2.00	2.00	1.20	1.20
5	6.60	6.70	3.30	3.28	1.80	1.87
−4	10.50	10.80	4.80	4.80	2.50	2.60
−13	—	—	6.60	6.61	3.40	3.40
−22	—	—	8.80	8.90	4.30	4.30
−31	—	—	—	—	5.35	5.48

[a]Calculated times (in seconds) for the shield-ice surface to reach 32°F from the initial temperature.

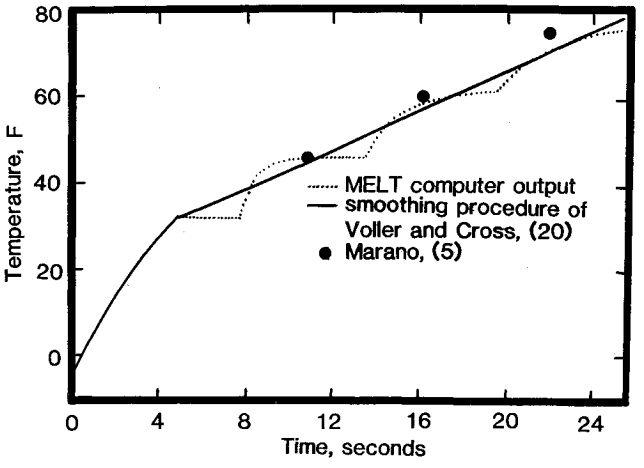

Fig. 3 Ice/abrasion shield interface temperature during phase change.

starting assumptions and therefore require additional iterations. Clearly, the computer time escalates as the number of these iterations increases. On the other hand, if the phase of each node were known prior to the start of the time step calculation, an efficient matrix inversion procedure could be used.

Schneider and Raw[21,22] have developed a technique that makes the direct solution of the system of equations for the Stefan problem possible. This method was incorporated into the analysis and produced a tridiagonal system of equations. This set of equations was then solved by Gaussian elimination, which is also known as the Thomas algorithm.

The Method of Assumed States

The method developed by Schneider and Raw may still require iterations as the calculation progresses, but the number of such iterations was found to be significantly smaller than the number of iterations using the Gauss-Seidel procedure. In this new method, the state of each node was assumed at the start of a time step and held fixed during the calculation for the new solution. On the basis of the previous nodal states and the new solution, a correction was made to the phase of each node and another solution sought. Usually only one to three such iterations were required to obtain a converged result in a given time step.

Two rules were used to establish the state of a node within a control volume. (The state of the node may be solid, phase transition, or liquid.) The two rules are:

1) In a single iteration, any given control volume is allowed to change by only one state. For example, in heating, a node is only allowed to change from solid to phase transition or from phase transition to liquid in a single iteration. A node control volume may not directly change from solid to liquid.
2) In a single iteration, the state of a control volume will not change if in the previous iteration its state and that of its neighbors was the same. For example, if the control volume under consideration and both its neighbors were solid, but the calculations predict its state should be liquid, the state of the control volume will be maintained as solid.

These two rules were developed to reflect the physical situation of a phase change in a melt process.

Results and Discussion

Several example problems were investigated using the computer program MELT, which was developed from the methodology previously presented. A baseline deicer design was used for all test cases. Results were compared to predictions obtained using the computer code developed by Marano.[5] The baseline model had convective heat transfer coefficients of 1.0 and 10^6 Btu/h-ft-°F specified at the substrate/ambient and the ice/ambient surfaces, respectively. Specific information concerning each of the layers in the pad is listed in Table 1.

The effect of the initial temperature of the composite and the heater power output on the time for the shield/ice interface to reach 32°F is shown in Table 2. For this case, the heater was turned on at time zero and then operated continuously thereafter. Power outputs of 15, 25, and 40 W/in.^{2} and initial temperatures from +23 to −31°F were investigated. As the table indicates, the results of the current code agree almost perfectly with the values obtained using the code developed by Marano.[5] This is to be expected, since for this problem there is no phase change and, as such, the problem is simply transient heat conduction through a multilayered body.

As a further comparison, a deicer pad with a 25 W/in. heater was analyzed for an operational time of 25 s. This length of time was selected in order to assure that the ice layer would begin to melt. The initial temperature of the pad was −4°F. The temperature variation of the shield/ice interface

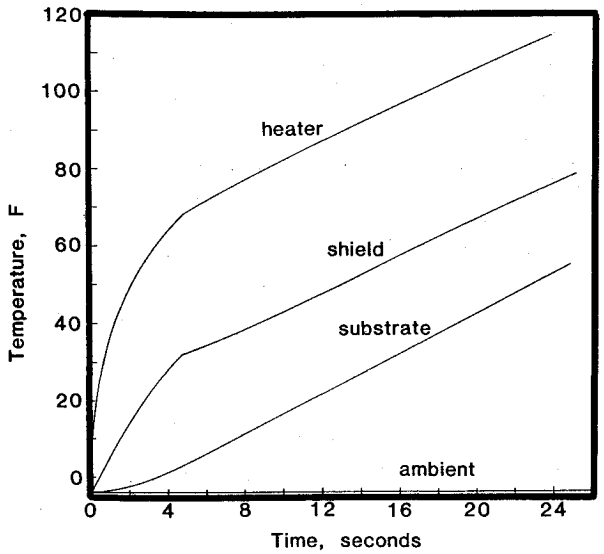

Fig. 4 Deicer temperature with continuous heating and no ice shedding.

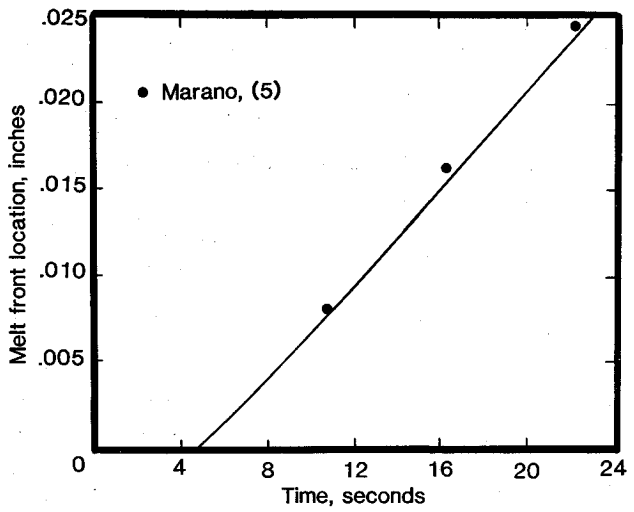

Fig. 5 Melt front location measured from the abrasion shield surface.

with time is shown in Fig. 3. The dashed curve represents the calculated results from the current program. The results display a periodic plateauing of the temperature as each nodal volume undergoes phase transition and melts. This result is not physically accurate, but is an outcome of the application of the enthalpy method, as discussed by Voller and Cross.[20] Applying their smoothing procedure removes the oscillatory temperature variations and produces the condituous curve shown. The results from Marano's code are also shown and it is seen that they are in good agreement with the current predictions. The slight differences are thought be to a result of the different finite-differencing schemes employed between the two, i.e., Marano used the Crank-Nicolson method, whereas a fully implicit method was used in the current study.

The size of the temperature plateaus in Fig. 3 can be altered by changing the number of nodes in the ice layer. An increased number of nodes decreases the plateau size (i.e., the length of time a node is at a fixed temperature). In the limit, a very large number of nodes should cause the dashed curve in Fig. 3 to approach the solid curve. This behavior is a result of modeling a continuous phase change process by a discretized numerical model.

Table 3 Comparison of CPU times

Point when calculations were terminated	Initial temperature 23°F Marano CPU / MELT CPU	Initial temperature −13°F Marano CPU / MELT CPU
Shield temperature reached 32°F	11.2	13.0
First ice node control volume is entirely melted	10.6	11.8

The data shown in Fig. 3 also reveal that the temperature history of a given location (in this case the shield/ice interface) oscillates less about the true value as the phase change front moves away from that location. This is indicated by the large differences between the two curves shown for times of 5–11 s and smaller variations for times over 20 s.

Temperatures at other locations in the baseline deicer pad after melting of the ice layer has commenced are shown in Fig. 4. The curve for the shield/ice interface is the same as that presented in Fig. 3. The heater temperature curve had oscillations (not shown) similar to those at the shield/ice interface, but the differences between them and the smooth curve were less. No oscillations in the temperature of the substrate were detected, because the substrate is far removed from the location where the phase change occurs.

The location of the phase change front as a function of time is shown in Fig. 5. The circles in the figure are results from the reference code. Agreement between the results is very good. As can be seen, no melting occurs until 4.8 s, after which melting takes place in nearly a linear manner. After 23 s, 0.025 in. of the ice has melted.

A comparison of the CPU times between Marano's code[5] and MELT is given in Table 3. The ratios of the CPU times for four different cases are presented. In each of the cases, the baseline deicer pad design was used. Two initial temperatures were considered: +23 and −13°F. For each of these temperatures, the calculations were terminated when 1) the shield/ice interface reached 32°F, but no melting occurred, and 2) the first nodal control volume in the ice layer became totally liquid. In each case, the CPU times for the current code were less than the reference code by at least a factor of 10. The very short running time for the current code is due to the efficient matrix inversion procedure used to solve the linear system of equations, assuming the state of each node in the two-phase region allows the use of the matrix inversion method. Only an occasional iteration is required when a node changes phase during a time step. By contrast, the reference code used the Gauss-Siedel iteration procedure for each time step regardless if the ice is melting or not.

Conclusions

A new aproach to calculate the transient thermal behavior of an iced multilayer electrothermal deicer pad was developed. The impetus of this work was the desire to employ methods that would greatly speed the computational times of numerical models of this structure and thereby produce more effective design tools.

The new approach focused on improved numerical treatment of the heat transfer in the internal pad layers, as well as on the phase change of the ice. A cubic spline technique was utilized to solve the internal layer heat transfer problem. By this approach, a set of algebraic equations having a tridiagonal form was established. This set was directly solved by Gaussian elimination. The computations were also made more efficient over previous models by eliminating the iterative procedure generally found in phase change problems. A modified enthalpy method was used in which the phase of each node in the ice layer was assumed at each time step. The

assumptions were based on two rules that effectively incorporate the physics of the melting process into the problem. What is more, these assumptions permit the ice layer equations to also be written in tridiagonal form and thereby allow a rapid inversion.

Comparisons were made to results obtained using an existing computer code. It was found that the current method consistently predicted temperatures that were in excellent agreement with those obtained using the reference code. Moreover, the computer run times were significantly reduced. The results indicate that CPU times were reduced by at least a factor of 10.

Although the problem solved was one-dimensional, it is believed that tremendous gains in reducing the overall computational times of the geometrically more complete, two-dimensional models can readily be made. This work is now being undertaken.

Appendix: Cubic Spline Relationships

A spline is a polynomial used for approximating a function, $u(x)$, over a portion of an interval that has been divided into n subintervals, not necessarily of equal length. The interfacial points between the subintervals are called the nodes and designated as x_j. If we wish to interpolate the function between the nodes, an interpolating polynomial may be used. An alternative to writing a single polynomial of degree n for the entire interval is to approximate the function by n polynomials called splines, one spline for each subinterval. By this approach, oscillation of the interpolating polynomial, which can occur between the interpolating points, is reduced.

Cubic splines are the most widely used splines, perhaps because of their simplicity and because they possess continuous first and second derivatives everywhere in the subinterval. The spline function will be designated here as $S(x)$. Since $S(x)$ is piecewise cubic, $S'(x)$ is piecewise quadratic and $S''(x)$ is piecewise linear and continuous. From Fig. A1a, an interpolating equation for $S''(x)$ is readily written as

$$S''(x) = M_{j-1}\left(\frac{x_j - x}{h_j}\right) + M_j\left(\frac{x - x_{j-1}}{h_j}\right) \tag{A1}$$

where $h_j = x_j - x_{j-1}$ and $S''(x_j) = M_j$, $j = 0,1,2,\ldots J$. Equation (A1) can be integrated twice to obtain $S(x)$, i.e.,

$$S(x) = \frac{K_1}{6}(x_{j-x})^3 + a_j(x_j - x) + \frac{K_2}{6}(x - x_{j-1})^3 + b_j(x - x_{j-1}) \tag{A2}$$

where $K_1 = M_{j-1}/h_j$, $K_2 = M_j/h_j$, and a_j and b_j are integration constants that can be found from the subinterval end conditions: $S(x_j) = U_j$ and $S(x_{j-1}) = U_{j-1}$. Performing this evaluation, inserting the coefficients into Eq. (A2), and differentiating the result produces

$$S'(x) = -\frac{M_{j-1}}{2h_j}(x_j - x)^2 + \frac{M_j}{2h_j}(x - x_{j-1})^2 + \frac{U_j - U_{j-1}}{h_j} - \frac{h_j}{6}(M_j - M_{j-1}) \tag{A3}$$

Evaluating this expression at $x = x_j$, then increasing the index of all variables in Eq. (A3) and evaluating that expression at $x = x_{j+1}$, gives the following two expressions for $S'(x)$ on either side of x_j, as illustrated in Fig. A1b

$$S'(x_j^-) = \frac{h_j}{6}M_{j-1} + \frac{h_j}{3}M_j + \frac{U_j - U_{j-1}}{h_j} \tag{A4}$$

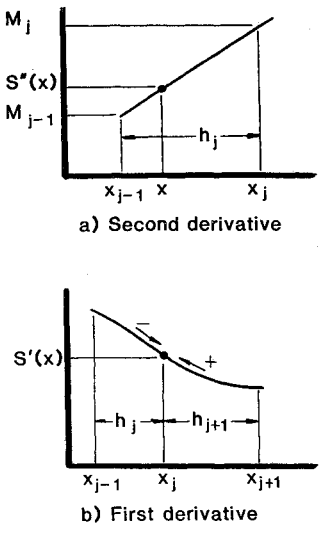

Fig. A1 Cubic spline derivative relationships.

$$S'(x_j^+) = -\frac{h_{j+1}}{3}M_j - \frac{h_{j+1}}{6}M_{j+1} + \frac{U_{j+1} - U_j}{h_{j+1}} \tag{A5}$$

Since $S'(x)$ is continuous, Eqs. (A4) and (A5) may be equated, which produces the following

$$\frac{h_j}{6}M_{j-1} + \left(\frac{h_j + h_{j+1}}{3}\right)M_j + \frac{h_{j+1}}{6}M_{j+1} = \frac{U_{j+1} - U_j}{h_{j+1}} - \frac{U_j - U_{j-1}}{h_j} \qquad j = 1,2,\ldots,J-1 \tag{A6}$$

Acknowledgments

Numerical work on the electrothermal deicer pad has been supported by the NASA Lewis Research Center, Cleveland, OH, Grant number NAG 3-72. The authors gratefully acknowledge this continuing support and the encouragement of their work by the grant monitor, Dr. R. J. Shaw.

References

[1]Marano, J. J., "Numerical Simulation of an Electrothermal Deicer Pad," M. S. Thesis, Univ. of Toledo, Toledo, OH, 1982.

[2]Stallabrass, J. R., "Thermal Aspects of Deicer Design," International Helicopter Icing Conference, Ottawa, Canada, 1972.

[3]Baliga, G., "Numerical Simulation of One-Dimensional Heat Transfer in Composite Bodies with Phase Change," M. S. Thesis, Univ. of Toledo, Toledo, OH 1980.

[4]Gent, R. W. and Cansdale, J. T., "One-Dimensional Treatment of Thermal Transients in Electrically De-Iced Helicopter Rotor Blades," Royal Aircraft Establishment TR 80159, Dec. 1980.

[5]Marano, J. J., "Numerical Simulation of an Electrothermal Deicer Pad," NASA CR-168097, March 1983.

[6]Leffel, K. L., Masiulaniec, K. C., De Witt, K. J., and Keith, T. G., "A Numerical and Experimental Investigation of Electrothermal Aircraft Deicing," *Proceedings of the 42nd Meeting of the American Helicopter Society,* American Helicopter Society, Alexandria, VA, June 1986, pp. 917-930.

[7]De Witt, K. J., Keith, T. G., Chao, D. F., and Masiulaniec, K. C., "Numerical Simulation of Electrothermal Deicing Systems," AIAA Paper 83-0114, Jan. 1983.

[8]Chao, D. F., "Numerical Simulation of Two-Dimensional Heat Transfer in Composite Bodies with Application to Deicing of Aircraft Components," Ph.D. Dissertation, Univ. of Toledo, Toledo, OH, 1983.

[9]Keith, T. G., Masiulaniec, K. C., De Witt, K. J., and Chao, D. F., "Predicted Electrothermal Deicing of Aircraft Blades," AIAA Paper 84-0110, Jan. 1984.

[10]Masiulaniec, K. C., Keith, T. G., De Witt, K. J., and Leffel, K. L., "Full Two-Dimensional Transient Solutions of Electrothermal Aircraft Blade Deicing," AIAA Paper 85-0413, Jan. 1985.

[11]Masiulaniec, K. C., Keith, T. G., and De Witt, K. J., "Finite Difference Solutions of Heat Conduction Problems in Multi-Layered Bodies with Complex Geometries," Paper 84-HT-58, 22nd ASME/AIChE National Heat Transfer Conference, Niagra, NY, July 1984.

[12]Ahlberg, J. H., Nilson, E. N., and Walsh, J. L., *The Theory of Splines and Their Application,* Academic, New York, 1967.

[13]Davis, P. J. and Rabinovitz, P., *Methods of Numerical Integration,* Academic, New York, 1975, pp. 50–56.

[14]Papamichael, N. and Whiteman, J. R., "A Cubic Spline Technique for the One-Dimensional Heat Conduction Equation," *Journal of the Institute for Mathematics and Its Applications,* Vol. 11, 1973, pp. 111–113.

[15]Rubin, S. G. and Graves, R. A., Jr., "A Cubic Approximation for Problems in Fluid Mechanics," NASA TR R-436, Oct. 1975.

[16]Lin, S., Wang, P., and Kahawita, R., "Cubic Spline Numerical Solution of an Abalation Problem with Convective Backface Cooling," *AIAA Journal,* Vol. 22, Aug. 1984, pp. 1176–1177.

[17]Arpaci, V. S., *Conduction Heat Transfer,* Addison-Wesley, Reading, MA, 1966, pp. 129–132.

[18]Shamsunder, N. and Sparrow, E. M., "Analysis of Multi-Dimensional Conduction Phase Change via the Enthalpy Model," *ASME Journal of Heat Transfer,* Vol. 97, 1975, pp. 333–340.

[19]Voller, V. R., "Implicit Finite-Difference Solutions of the Enthalpy Formulation of Stefan Problems," *IMA Journal of Numerical Analysis,* Vol. 5, 1985, pp. 201–214.

[20]Voller, V. R. and Cross, M., "Accurate Solutions of Moving Boundary Problems Using the Enthalpy Method," *International Journal of Heat and Mass Transfer,* Vol. 24, 1981, pp. 545–556.

[21]Schneider, G. E. and Raw, M. J., "An Implicit Solution Procedure for Finite Difference Modeling of the Stefan Problem," *AIAA Journal,* Vol. 22, Nov. 1984, pp. 1685–1690.

[22]Raw, M. J. and Schneider, G. E., "A New Implicit Solution Procedure for Multidimensional Finite-Difference Modeling of the Stefan Problem," *Numerical Heat Transfer,* Vol. 8, 1985, pp. 559–571.

[23]Roelke, R. J., "A Rapid Computational Procedure for the Numerical Solution of a Heat Flow Problem with Phase Change," M. S. Thesis, Univ. of Toledo, Toledo, OH, 1986.